Resonance Raman Spectroscopic Characterization of the Molybdopterin Active Site of DMSO Reductase[†]

L. Kilpatrick,[‡] K. V. Rajagopalan,[§] J. Hilton,[§] N. R. Bastian,[§] E. I. Stiefel,[||] R. S. Pilato,[⊥] and T. G. Spiro*[‡]

Department of Chemistry, Princeton University, Princeton, New Jersey 08544, Department of Biochemistry,
Duke University School of Medicine, Durham, North Carolina 27710, EXXON Research and Engineering Company,
Clinton Township Route 22 East, Annandale, New Jersey 08801, and Department of Chemistry, University of Maryland,
College Park, Maryland 20742

ABSTRACT: Resonance Raman spectra are compared for *Rhodobacter sphaeroides* dimethyl sulfoxide reductase, an enzyme containing a molybdopterin cofactor, and two model compounds, **I** and **II**, which have pterin and quinoxaline, respectively, attached to a $Cp_2Mo[IV]$−dithiolene chelate [Cp = cyclopentadienyl]. The effect of ^{34}S incorporation was also determined. Several bands in the 200−500 cm^{-1} region show remarkably similar patterns of frequencies and isotope shifts between protein and models: a band at 351 cm^{-1} shifts 6−8 cm^{-1}, and bands at lower and higher frequencies show smaller shifts upon ^{34}S substitution. A normal coordinate analysis on **II** indicates the 351 cm^{-1} mode to be the symmetric Mo−S[dithiolene] stretch and the remaining low-frequency modes to contain contributions from deformations of the quinoxaline ring as well as from Mo−S stretching. The similarity in the low-frequency spectra between the model compounds and the enzyme strongly supports a dithiolene chelate as the mode of Mo−pterin interaction in the cofactor. Resonance enhancement of both high- and low-frequency quinoxaline or pterin modes is observed for both model compounds, implicating the heterocyclic rings as part of the electronic system involved in the Mo−dithiolene charge transfer transitions. RR spectra of 6-methylpterin and biopterin are reported and used to identify the pterin and quinoxaline high-frequency bands in the model compound spectra. The dithiolene C=C stretch is tentatively assigned to bands at 1506 cm^{-1} in **I** and 1515 cm^{-1} in **II**. The RR spectrum of the oxidized protein contains a strong band at 1576 cm^{-1}, a moderate intensity band at 1526 cm^{-1}, and several weaker bands. Denaturation experiments indicate the pterin to be at the dihydro oxidation level. It is proposed that the pterin is in the 5,8-dihydro form, in which the dithiolene C=C bond is conjugated with the C(6)=C(7) bond of the pterin, and that the 1526 and 1576 cm^{-1} bands arise from the coupled stretches of these two double bonds.

With the exception of nitrogenase (Kim & Rees, 1992) molybdenum is found in enzymes as part of a pterin-containing cofactor (Johnson et al., 1980). These enzymes catalyze two-electron redox reactions and can be prepared with the Mo in oxidation states VI, V, and IV. EXAFS measurements have established at least one Mo=O bond for all three oxidation levels (Cramer, 1983). The Mo[VI]-containing enzymes have an additional M=O (George et al., 1989, 1990; Cramer et al., 1984), or Mo=S bond (Hille et al., 1989; Turner et al., 1989; Bordas et al., 1980; Cramer & Hille, 1985; Cramer et al., 1979, 1981; Branzoli & Massey, 1974), which is converted to Mo-OH or Mo-SH in the Mo-[V] and Mo[IV] states. These redox changes are undoubtedly involved in the enzymatic mechanisms, which may involve oxo-transfer reactions to and from the Mo (Hille & Sprecher, 1987). Model chemistry for these reactions has been extensively developed (Holm, 1990).

The Mo−pterin cofactor can be extracted from molybdoproteins and the extract is able to reconstitute nitrate reductase activity in a cofactor-deficient mutant, *nit-1*, of *Neurospora crassa* (Nason et al., 1971; Rajagopalan, 1991). The extracted cofactor is extremely labile and has eluded direct structural characterization. Chemical studies (Johnson et al., 1984; Johnson & Rajagopalan, 1982; Kramer et al., 1987), however, have led to the proposed structure shown in Figure 1, in which Mo is bound to the pterin through a side chain bearing a novel dithiolene chelate. In the case of the enzyme dimethyl sulfoxide reductase (DR), from *Rhodobacter sphaeroides* (Satoh & Kurihara, 1987; Bastian et al., 1991), the cofactor contains molybdopterin guanine dinucleotide (MGD), in which the pterin side chain is attached to 5'-GMP through a pyrophosphate linkage (Johnson et al., 1990). Mo−pterin cofactor characterization is facilitated in DR by the absence of additional cofactors (iron−sulfur, heme, flavin), which are found in other Mo enzymes. The oxidized form of DR contains Mo(VI), while the reduced form contains Mo(IV). Model compounds, also shown in Figure 1, have recently been synthesized in which Cp_2Mo-[IV] (Cp = cyclopentadienyl) is bound to dithiolene which is attached to either pterin or quinoxaline in the same manner as is proposed for the cofactor (Pilato et al., 1993). The structure has been confirmed for the quinoxaline compound by X-ray crystallography (Pilato et al., 1991).

The role of the pterin in the functioning of the cofactor is not understood. While pterins are redox cofactors in their

* Author to whom correspondence should be addressed.
[‡] Princeton University.
[§] Duke University School of Medicine.
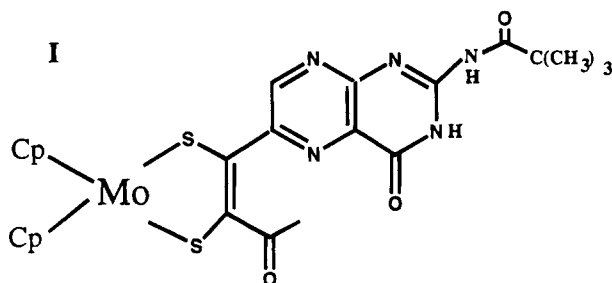[||] EXXON Research and Engineering Co.
[⊥] University of Maryland.
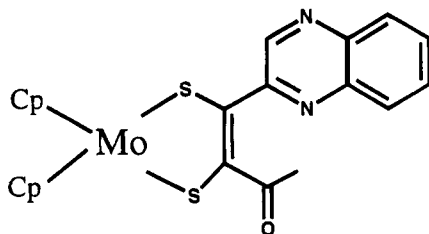
MPT
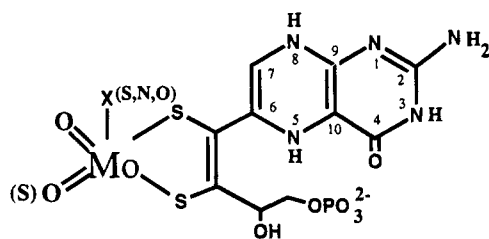
I

II

FIGURE 1: Proposed structures for the molybdopterin cofactor (MPT) (the pterin is shown in the proposed 5,8-dihydro form; in DR the phosphate group is replaced by GDP) and for the two model complexes $Cp_2Mo(IV)S_2C_2(C(O)Me)$-(C-6 pterin) (**I**) and Cp_2Mo-$(IV)S_2C_2(C(O)Me)$-quinoxaline (**II**). (Cp = cyclopentadienyl).

own right in a variety of enzyme systems, there is no evidence for or against pterin redox changes in the accessible states of Mo−pterin enzymes. Denaturation experiments involving difference spectra and redox titrations indicate that the pterin is at the dihydro oxidation level in the Mo[VI] forms of the proteins (Gardlik & Rajagopalan, 1990). There are several possible dihydro tautomers, and only the stable 7,8-dihydro form has been isolated [although other unstable forms are isolable for substituted pterins and pteridenes (Randles & Armarego, 1985; Matsura et al., 1986; Brown, 1988)]. The denaturation experiments suggested that this is not the form present in the cofactor and indeed that different forms may be present in different proteins (Gardlik & Rajagopalan, 1990).

DR is an attractive vehicle for *in situ* characterization of the cofactor by spectroscopic methods, because, unlike other Mo−pterin enzymes, it contains no interfering chromophores, e.g., Fe-S clusters, flavin, or heme. Optical absorption spectra are available for the Mo[VI] and [IV] states (Satoh & Kurihara, 1987; Bastian et al., 1991), and the Mo[V] optical transitions in a glycerol-inhibited form of the enzyme have recently been characterized by absorption, CD, and variable temperature MCD spectroscopy (Finnegan et al., 1993). We have reported a preliminary investigation of the Mo[VI] and Mo[IV] states using resonance Raman (RR)

spectroscopy, which lent support to the dithiolene chelate model (Gruber et al., 1991). In this study, we have extended the RR characterization significantly and strengthened the spectral interpretation with the aid of the newly available model compounds.

EXPERIMENTAL PROCEDURES

Materials. 6-Methyl pterin, biopterin, and pterin were purchased from Aldrich Chemical Co. 6-Methyl-7,8-dihydropterin was prepared according to the methods of Viscontini (1971), and $Cp_2Mo(IV)S_2C_2(C(O)Me)$-(C-6 pterin) (**I**) and $Cp_2Mo(IV)S_2C_2(C(O)Me)$quinoxaline (**II**) were prepared as described previously (Pilato et al., 1991, 1993).

DR from *R. sphaeroides* was purified to homogeneity by a modification (Bastian et al., 1991) of the method of Satoh and Kurhara (1987). The oxidized Mo(VI) form of the enzyme was reduced to the Mo(IV) form with sodium dithionite. Excess dithionite was removed by anaerobic gel (PD-10) chromatography. Specific activity [16 μmol of DMSO reduced/(min·mg)] was established by monitoring the substrate-dependent oxidation of reduced benzyl viologen in 50 mM Tris-HCl, pH 7.5. The ^{34}S containing protein was prepared by growing *R. sphaeroides* on ^{34}S (Bastian et al., 1991).

Resonance Raman Spectroscopy. Resonance Raman spectra were obtained using a 135° back-scattering geometry. Frozen solutions of DR (79 mg/mL, in 50 mM Tris-HCl at pH 7.5), and solid samples (KCl pellets) of **I** and **II** were mounted on the tip of a copper finger which was then cooled to liquid nitrogen temperatures. This technique minimizes laser-induced decomposition and provides high-quality spectra from small samples (Czernuszewicz & Johnson, 1983). The dithionite-containing DR sample was loaded onto the sample cell in an O_2-free glove box. The sample cell was then sealed under an N_2 atmosphere and cooled to 77 K. RR spectra of CH_2Cl_2 solutions of **I** and **II** ($\sim$2 mM) were obtained at room temperature by back-scattering from spinning NMR tubes. The RR spectrum of a THF solution of **II** at 11 K was collected by mounting the sample on the cold finger of a Model CSA-202E closed-cycle liquid He refrigerator (Air Products, Allentown, PA) (Czernuszewicz, 1986). In this experiment, the scattered light was collected in a 180° back-scattering geometry. The RR spectra of the pterin derivatives were obtained from spinning solid samples (KCl pellets) at room temperature.

RR excitation was provided with a Coherent Innova 100-K3 Kr^+ laser or a Spectra Physics Ar^+-pumped dye laser (LDS 722). The scattered radiation was dispersed by a 1877 Spex triplemate and detected with either a Princeton Instruments image-intensified diode array or a Photometrics charge coupled device (CCD), cooled to −30 and −102 °C, respectively. The average laser powers for collecting protein, analogs, and pterin samples were 80, 50, and 20 mW, respectively. The RR spectra of pterins were obtained by dispersing the scattered radiation through an 1877 Spex triplemate equipped with UV coated mirrors and 2400-groove/mm gratings blazed at 250 nm. The light was detected using a Princeton Applied Research intensified diode array. For 7,8-dihydrobiopterin, the laser power was further reduced to <10 mW, and a defocused laser beam was used to minimize the extent of photooxidation.

The RR spectra were processed using Labcalc software (Galactic Industries Corp.). The data were calibrated using

the known vibrational frequencies of carbon tetrachloride, dimethylformamide, and indene. The RR spectra of the natural abundance and [34]S-labeled samples were always taken on the same day (using the same calibration) to increase the accuracy of the observed isotopic shifts. Vibrational bands associated with the plastic sample holder used in the DR experiments were subtracted from the RR spectra.

The normal mode analysis of **II** was carried out using the GF matrix method (Wilson et al., 1955). Schachtschneider's programs were employed to construct the G matrices and to solve the secular equation (Schachtschneider, 1962). The Cartesian coordinates used in the calculation were taken from the X-ray crystal structure coordinates (Pilato et al., 1991). The cyclopentadienyl (Cp) rings were included as point masses. A Urey Bradley force field was used to calculate the observed frequencies and [34]S isotope shifts.

RESULTS

RR spectra were obtained with laser excitation at wavelengths within the long-wavelength absorption bands of the protein and model compounds. Excitation at 676.4 nm was used for the protein [λ_{max} = 720 and 630 nm for the oxidized and reduced forms (Gruber et al., 1991)], while 530.8 nm excitation was used for the models (λ_{max} = 500 nm). An exitation profile determined for **II** (data not shown) established that the enhancement is resonant with the long wavelength electronic transition.

Mo=O stretching vibrations are expected between 850 and 1000 cm^{-1}. A careful search of this region of the protein RR spectra was carried out, but although weak bands were seen, none of them shifted when the enzyme was cycled in H$_2$[18]O between redox levels, a procedure that should label the oxo groups. A study of the oxodithiolene model complex Mo^{IV}O[S$_2$C$_2$(CO$_2$Me)$_2$]$_2^{2-}$ located the M=O stretch at 910 cm^{-1} with laser excitation at 568.2 nm, in the long-wavelength absorption band (Subramanian et al., 1990). The intensity was very low, however, and it is not surprising that the protein samples do not show M=O scattering under comparable conditions. RR bands were, however, detected at low frequencies, in the region of Mo−S stretching vibrations and at high frequencies in the region of pterin ring modes.

(1) Low-Frequency Modes. RR spectra between 250 and 450 cm^{-1} are shown in Figure 2 for frozen solutions (77 K) of oxidized and reduced protein, DRox and DRred, obtained from bacteria grown on natural abundance or [34]S. The DRox spectra are in good agreement with those reported previously (Gruber et al., 1991). Slight differences with respect to the previously reported DRred spectra (Gruber et al., 1991) may be attributed to incomplete reduction of the earlier sample. Metal−ligand stretching vibrations are expected in this frequency region. Large (7−8 cm^{-1}) [34]S shifts are seen for bands that appear at the same frequency, 350 cm^{-1}, in both oxidation states. These bands are clearly associated with Mo−S stretching. Lesser shifts, 2−6 cm^{-1}, are seen for several other bands of both spectra. Thus, other vibrational modes of the chromophore mix with the Mo−S stretches and are resonance enhanced.

Figures 3 and 4 show low-frequency RR spectra of solid samples (77 K) of the pterin (**I**) and quinoxaline (**II**) model complexes and their [34]S isotopomers. There is a striking homology with the protein spectra in respect to frequencies

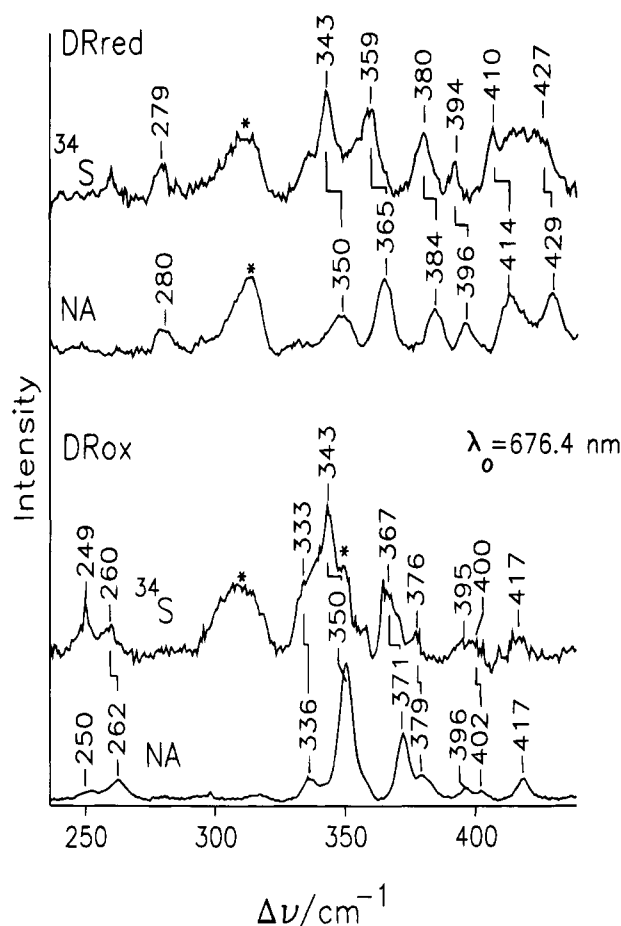FIGURE 2: RR spectra (77 K) of DRox and DRred obtained with 676.4 nm excitation in the 250−450 cm^{-1} region. The spectrum of natural abundance protein is compared with the spectrum of protein from bacteria grown on [34]SO$_4^{2-}$. Asterisks mark the ice band at ~310 cm^{-1}. In the RR spectrum of [34]S labeled Drox, the asterisk at ~350 cm^{-1} also marks the band of residual unexchanged dithiolene sulfur groups. Conditions: 60 mW laser power, 4 cm^{-1} slit width, triple spectrograph with CCD detector.

and [34]S isotope shifts. Shifts of 7−8 cm^{-1} are seen for bands at 348 cm^{-1} in **I** and at 351 cm^{-1} in **II**. The spectra are rich in features, and several other bands show significant [34]S shifts. There is a close correspondence of frequencies and isotope shifts between the model compounds and the proteins, as shown in Table 1. The relative intensities, however, are quite different. The strongest bands in the protein spectra are those showing the largest [34]S shifts, but these are of only moderate intensity in the model compound spectra, whereas the strong bands of the model compounds show small isotope shifts and are weak in the protein spectra. To some extent, however, this intensity pattern is a function of the state of the model compound samples. We observed marked changes in the relative intensities pattern, and also some frequency shifts, when **II** was dissolved in tetrahydrofuran and also when this solution was cooled to 11 K (data not shown). These changes probably reflect alterations in vibrational mode mixing occasioned by changes in molecular conformation, especially with respect to rotations about the bonds connecting the dithiolene with the quinoxaline and carbomethoxy groups (Figure 1).

To gain more insight into the nature of these low-frequency modes, we carried out a normal mode calculation on **II**. The structure parameters were taken from the crystal structure (Pilato et al., 1991), and the force constants (Table 2) were
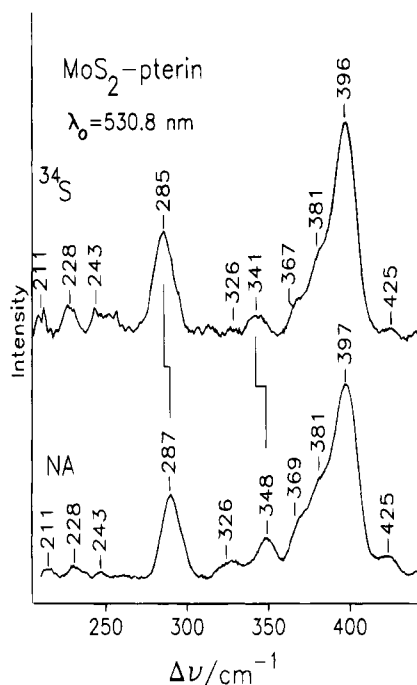
FIGURE 3: RR spectra with 530.8 nm excitation for the pterin model compound **I** (KCl pellet, 77 K) and its [34]S isotopomer in the 200–450 cm^{-1} region. Conditions: 4 cm^{-1} slits, 60 mW laser power; scanning spectrometer advanced in 0.5 cm^{-1} increments.
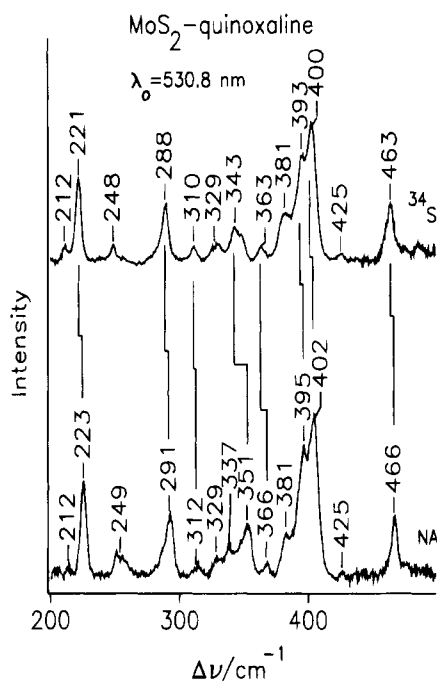

FIGURE 4: RR spectra with 530.8 nm excitation for the quinoxaline model compound **II** (KCl pellet, 77 K) and its [34]S isotopomer in the 200–450 cm^{-1} region. Conditions are as given in the legend to Figure 3.

adapted from studies of related molecules [naphthalene (Scully & Whiffen, 1960) and thiomolybdate (Müller et al., 1985)]. Table 3 compares the observed and calculated frequencies and [34]S shifts. The agreement is satisfactory. It is notable that the calculation spreads the isotope shifts among several modes as is seen in the experimental shifts. The potential energy distribution indicates a heavy involvement in these modes of quinoxaline deformations, both in an out of the plane of the ring.

Table 1: RR Band Frequencies (cm^{-1}) and [34]S Isotope Shifts (Parentheses) of Cp$_2$Mo(IV)S$_2$C$_2$(C(O)Me)-quinoxaline and Cp$_2$Mo(IV)S$_2$C$_2$(C(O)Me)-pterin (at 77 K in KCl Pellets) and of DMSO Reductase in the Oxidized (DRox) and Reduced (DRred) Forms (77 K Frozen Solutions)

MoS$_2$-quinoxaline	MoS$_2$-pterin	DRox	DRred
483 (3)			
466 (3)			
			429 (2)
425 (0)	425 (0)		
			414 (4)
402 (2)		402 (−)	
395 (2)	397 (1)	396 (−)	396 (2)
381 (0)	381 (0)		
		379 (3)	384 (4)
366 (3)	369 (2)	371 (4)	365 (6)
351 (8)	348 (7)	350 (7)	350 (7)
337 (−)		336 (3)	
329 (0)	326 (0)		
312 (2)			
291 (3)	287 (2)		
		262 (2)	
249 (1)	243 (0)	250 (1)	
223 (2)	228 (0)		
212 (0)	211 (0)		

Table 2: Urey Bradley Force Constants for Cp$_2$Mo(IV)S$_2$C$_2$(C(O)Me)-quinoxaline[a]

K(Mo−S)	1.32		
K(S−C)	3.30		
K(C=C)	5.40		
K(Mo−Cp)	2.58		
K(C−C)	4.80		
K(C=N)	5.60		
K(C=O)	8.00		
H(MoSC)	0.25		

H(SC=C)	0.82	H(CC=O)	1.10
H(CpMoS)	0.08	H(CCC)	1.10
H(CpMoCp)	0.08	H(O=CC)	1.10
H(SMoS)	0.08	H(C$_r$C$_r$N)	1.37
H(SCC(O))	0.82	H(C$_r$NC$_r$)	1.40
H(SCC$_r$)	0.82	H(C$_r$C$_r$C$_r$)	1.37
H(CC$_r$N)	1.10	H(CC$_r$C$_r$)	1.10
H(C=CC(O))	1.10	H(C=CC$_r$)	1.10

τ(SC=CS)[b]	0.16
τ_t(C=C)[c]	0.156
τ_c(C=C)	0.16
f(MoS,SC)	0.20
f(SC,SC=C)	0.35
f(MoS,SC=C)	0.10
f(MoS,SCC)	0.10
F(S−S)	0.10

[a] K = stretching (mdyne/Å); H = bending (mdyn·Å/rad^2); f = stretch−stretch (mdyne/Å) and stretch−bend interaction (mdyn/rad); F = nonbonded interaction (mdyn/Å); τ = torsion (mdyn/Å); C$_r$ = carbon of quinoxaline ring; C(O) = carbonyl group; Cp = cyclopentadienyl ring. [b] Torsion about the ditholene C=C bond. [c] Torsion about a C=C bond of the quinoxaline ring.

(2) High-Frequency Modes. In the 1300–1700 cm^{-1} region (Figure 5), DRox shows a prominent band at 1576 cm^{-1}, a moderately strong band at 1526 cm^{-1}, and weaker bands, at 1304, 1342, 1373, and 1656 cm^{-1}. The 1373 cm^{-1} band shifts down 18 cm^{-1} when the protein is incubated in D$_2$O, but there are no other changes. When the protein is reduced, the signal diminishes sharply. Two bands are seen in the DRred spectrum, at 1573 and 1342 cm^{-1}, but it is difficult to be sure that these are not simply remnant bands of a small amount of unreduced protein. In our preliminary report (Gruber et al., 1991) bands were reported at 1573 and

Table 3: Observed and Calculated[a] Frequencies and ^{34}S Isotope Shifts (cm^{-1}) for Cp$_2$Mo(IV)S$_2$C$_2$(C(O)Me)-quinoxaline

obsd	calcd	Δ^{34}S obsd	calcd	PED (%)[b]
483	483	3	1	36(NC$_r$C$_r$) + 13(C$_r$NC$_r$) + 11(S–C) + 12(CC$_r$N)
466	451	3	0	52(β)
425	420	0	0	11(C$_r$C$_r$C$_r$) + 19(NC$_r$C$_r$) + 25(β)
402	399	2	1	11(S–C) + 10(CC(O)C) + 30(β)
395	392	2	2	12(S–C) + 60(β)
381	381	0	0	98(Mo–Cp)
366	375	3	3	18(Mo–S) + 11(SCC) + 11(β) + 11(α)
351	353	8	7	64(Mo–S) + 13(Mo–Cp)
337	331		5	19(S–C)
329		0		
312	301	2	3	56(Mo–S) + 11(C$_r$C$_r$C$_r$) + 24(NC$_r$C$_r$)
291	298	4	2	98(β)
	280		2	80(Mo–Cp)
249	262	1	1	18(NC$_r$C$_r$)
223	230	2	1	25(β) + 34(α)
212	194	0	0	53(β)

[a] Includes all calculated frequencies between 200 and 500 cm^{-1}. [b] Percentage contribution of the indicated internal coordinate (stretch for a bond, bend for an angle formed by three atoms) to the potential energy; C$_r$ is a quinoxaline ring carbon. α = torsional motion about the dithiolene C=C; β = torsion involving the quinoxaline ring.
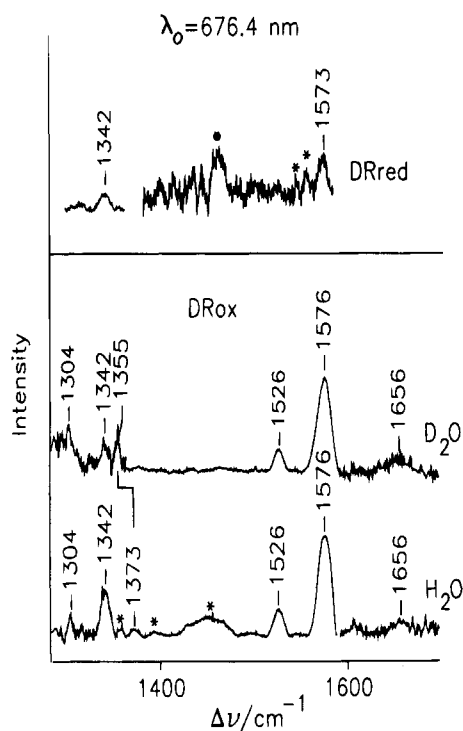
λ_o=676.4 nm

FIGURE 5: High-frequency RR spectrum of DRox in H$_2$O and D$_2$O and of DRred obtained with 676.4 nm excitation. Asterisks mark bands arising from the plastic sample holder. Conditions are as given in the legend to Figure 2.

1568 cm^{-1} for DRox and DRred, but the 1568 cm^{-1} DRred band has not been reproduced in subsequent measurements and must have been an artifact of the incompletely reduced sample.

Figure 6 shows the same spectral region for the model compounds (bottom two spectra). Several more bands are seen than in DRox, and there is rather good correspondence among the frequencies in the two spectra, although the relative intensities differ. As in the low-frequency region, the bands are noticeably broader for **I** than **II**.

To investigate the nature of the band pattern expected for pterins, we recorded RR spectra of 6-methylpterin [6-MePT]
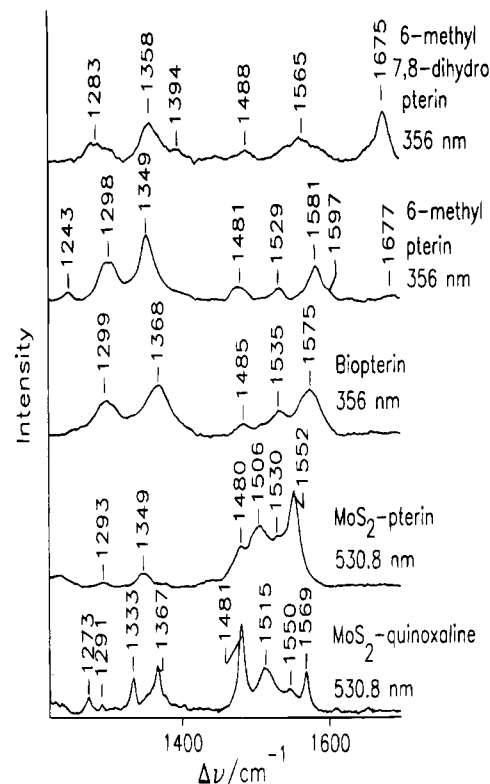

FIGURE 6: Comparison of high-frequency RR spectra of the pterin and quinoxaline model compounds with those of oxidized biopterin and 6-methylpterin and of the 7,8-dihydro form of 6-methylpterin. The latter three spectra were obtained with 356 nm excitation, near resonance with the UV electronic transitions.

and biopterin in their oxidized forms, and of 6-MePT in the 7,8-dihydro form, using 356 nm excitation, near resonance with the π–π^* electronic transitions. These pterins have simpler substituents, methyl and 1,2-dihydroxypropyl, respectively, at the same C6 position as the MPT side chain (Figure 1). Their spectra are compared in Figure 6 with those of **I** and of **II**. Figure 7 shows the effect on the oxidized 6-methylpterin spectrum of extracting the compound in DCl-containing D$_2$O, and reprecipitating it in neutral D$_2$O, a procedure that exchanges the N3H and C2-NH$_2$ protons (see Figure 1) for deuterons.

(3) Absorption Spectra of Anaerobically Denatured DR. In order to determine the pterin oxidation level, we performed absorption spectroscopy (Figure 8) on denatured samples of holoenzymes as described earlier in the case of sulfite oxidase and xanthine oxidase (Gardlik & Rajagopalan, 1990). DR (3.66 μM) was denatured in the presence of 6 M guanidine hydrochloride (GdnHCl$^-$, 1 mM EDTA, 10 mM Tris-Cl, pH 7.0) under anaerobic conditions, eliminating the absorption bands arising from molybdenum–dithiolene coordination without affecting the oxidation state of the pterin ring. Pterin-free apoprotein was placed in the reference cell to cancel the denatured protein absorbance. [The apoprotein was prepared by combining 100 μg of DR with 6 M GdnHCl and 1 mM EDTA, pH 7.0, under anaerobic conditions. Iodoacetamide (4.6 mg/mL) was included in the solution to alkylate the dithiolene thiols of the MGD rendering them unreactive (Kramer et al., 1987). The apoprotein was separated from the MGD on a column packed with Sephadex G-25 (fine) that was equilibrated with 6 M GdnHCl and 1 mM EDTA, pH 7.0, and was concentrated by ultrafiltration.] As shown in Figure 8, the difference spectrum (a) of
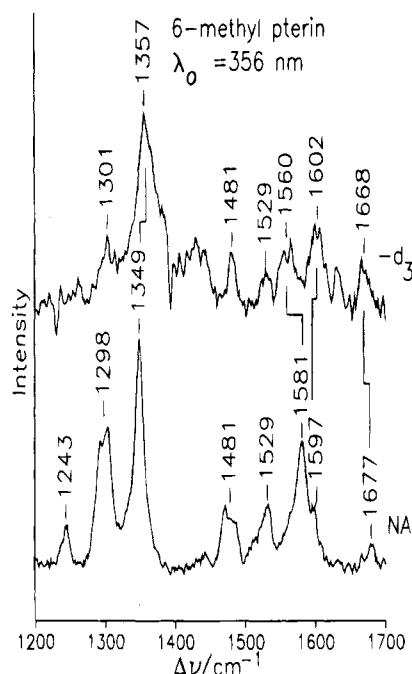
FIGURE 7: Effect on the RR spectra of 6-methylpterin of H/D exchange at the NH_2 and NH protons. Conditions: 356 nm laser excitation, 298 K. To prevent photodecomposition, the samples (KCl pellets) were mounted on a spinning Raman cell.
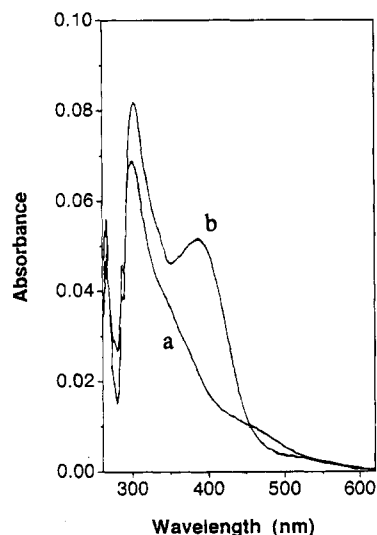

FIGURE 8: (a) Absorption spectrum of anaerobic denatured DR (see text for details) after subtraction of the spectrum of denatured apoprotein, showing a 300 nm peak attributed to a dihydropterin. (b) Same solution after air oxidation, showing the growth of a 385 nm band, characteristic of oxidized pterin.

denatured holo-DR versus the apoprotein has a peak at 300 nm. Upon subsequent oxidation of the sample in air, the difference spectrum (b) showed an absorption band at 385 nm due to the oxidation of the pterin.

Further evidence that the pterin ring of the molybdenum cofactor is in a dihydro state of reduction was provided by 2,6-dichlorobenzenoneindophenol (DCIP) reduction experiments similar to those described earlier with sulfite oxidase and xanthine oxidase (Gardlik & Rajagopalan, 1990). DR was denatured anaerobically in 6 M GdnHCl and 100 mM Tris-Cl, pH 7.0, in the presence of $HgCl_2$ to prevent reduction of the pterin by thiols. Oxidized DCIP was added anaerobically, and the change in the A_{600} of the sample was measured after 15 min. These experiments showed that

MGD in the native state is capable of two-electron reduction of DCIP. Finally, the difference spectrum of DR oxidized with an excess of DCIP (in 6 M GdCl, 2 mM EDTA, 0.1 mM $HgCl_2$, 50 mM potassium phosphate, pH 7.0), recorded versus a reference sample of native DMSO reductase in the same buffer, revealed an absorption band at 385 nm, demonstrating that, after two-electron oxidation by DCIP, the MGD was in the fully oxidized state.

DISCUSSION

(1) Pterin Ring Modes. The vibrational modes of the pterin ring have not been analyzed, but resonance with the $\pi-\pi^*$ transitions is expected to enhance modes in which the ring C—C and C—N bonds are stretched in the 1000—1700 cm^{-1} region. This is the region where RR bands of 6-MePT and biopterin are observed with excitation near their first UV absorption bands. Pterin is chemically similar to guanine; the main difference is that the pyrazine ring of pterin is replaced by an imidazole ring in guanine. The pterin UVRR spectra do in fact bear a resemblance to those of dGMP (Fodor et al., 1985). In particular, the highest frequency bands, at 1677 cm^{-1} for 6-MePT and 1679 cm^{-1} for dGMP, are readily assigned to the C4=O stretching vibration; they both shift down 9 cm^{-1} upon N(3)H/D exchange (Figure 7) due to the loss of the interaction with N—H bending. The D_2O-insensitive band at 1529 cm^{-1} in 6-MePT may be similar to the 1540 cm^{-1} D_2O-insensitive band of dGMP. On the other hand, the D_2O-sensitive 6-MePT bands at 1243 and 1298 cm^{-1} do not have correspondences in the dGMP spectra, and although the 1349, 1481, and 1581 cm^{-1} bands do have correspondences, they show different deuteration behavior in the two molecules. The 1349 cm^{-1} 6-MePT band shifts up 8 cm^{-1} in D_2O while a 1364 cm^{-1} dGMP band shifts down by the same amount; the 1481 cm^{-1} band is D_2O-insensitive in 6-MePT but shifts from 1489 to 1480 cm^{-1} in dGMP; and the 1580 cm^{-1} band is D_2O-insensitive in dGMP but shifts down 21 cm^{-1} in 6-MePT. In addition, a neighboring 1597 cm^{-1} band in 6-MePT, not seen for dGMP, shifts up 5 cm^{-1} in D_2O. Thus, the mode compositions of the heterocycles differ in detail.

Comparing RR spectra for oxidized 6-MePT and biopterin (Figure 6), we find a band-for-band correspondence (the 1677, 1597, and 1243 cm^{-1} bands are too weak to be seen in biopterin), although the frequencies differ by 5—20 cm^{-1}. These differences are surprising in view of the chemical similarity of the two pterins and suggest a significant degree of mechanical coupling between the ring modes and (unseen) substituent modes. When the spectrum of **I** is included in the comparison, there is again a band-for-band correspondence, except that **I** has an additional band at 1506 cm^{-1} and 6-methyl pterin has a weak band at 1597 cm^{-1}. The 1552 cm^{-1} band is considerably lower in frequency than the corresponding 1581 cm^{-1} band of 6-MePT. In view of the strong deuteration sensitivity of the latter, it seems likely that the frequency depression in **I** is due to the pivaloyl substituent on the C2 amino group (Figure 1). This substitution might have an uncoupling effect similar to H/D exchange. Surprisingly, in view of the chemical difference between pterin and quinoxaline [substitution of the pterin pyrimidine ring by benzene (Figure 1)], the band correspondences extend even to the spectrum of **II**, although extra bands now appear at 1273 and 1367 cm^{-1}, in addition to the extra 1515 cm^{-1} band, seen also in **I** (at 1506 cm^{-1}).

The spectrum of 7,8-dihydro-6-MePT has a distinctly different frequency and intensity pattern, as might be expected from the loss in aromaticity of the pyrazine ring and the consequent alteration in the conjugation pathway. Particularly striking is the intensification of the C=O stretching band at 1675 cm^{-1}. This band is very weak for oxidized pterins, but it is the strongest band in the 7,8-dihydro spectrum. Evidently, the C=O bond is much more strongly involved in the 7,8-dihydro conjugation path.

(2) Dithiolene C=C Stretch. The stretching vibration of the dithiolene double bond is expected in the 1300–1600 cm^{-1} region (Subramanian et al., 1990; Schläpfer & Nakamoto, 1975; Clark & Turtle, 1978). The frequency is variable, because of the availability of resonance forms corresponding to enedithiol and dithiene electronic structures. For example, the frequency decreases from 1534 to 1485 to 1425 cm^{-1} for the complexes $Ni[S_2C_2(CF_3)_2]_2^{z-}$, where $z = 2, 1,$ and 0, respectively, because the electrons are extracted successively from a HOMO that is bonding with respect to the C=C bonds (Schläpfer & Nakamoto, 1975). In the Mo-[IV] monooxo, bisdithiolene, $MoO[S_2C_2(CO_2Me)_2]_2^{2-}$, the C=C RR band was found at 1535 cm^{-1} (Subramanian et al., 1990). Since I and II are also Mo[IV] dithiolenes, it seems likely that the C=C stretch is among the group of four RR bands between 1480 and 1570 cm^{-1} (Figure 6). We tentatively assign the 1506 (I) and 1515 cm^{-1} (II) bands to this mode, since the other three bands find correspondences in the pterin spectra.

(3) High-Frequency DR Spectrum. The RR spectrum of DRox in the ring mode region (Figure 5) bears little resemblance to the oxidized pterin spectra (Figure 6), consistent with the conclusion from the anaerobic denaturation experiments that the pterin is at the dihydro oxidation level. Neither does the spectrum resemble that of the stable dihydro form, 7,8-dihydropterin (Figure 6). The anaerobic denaturation difference spectrum shows a band at 300 nm, closer to the wavelength expected for tetrahydropterin than for 7,8-dihydropterin. Unstable dihydro forms have been reported to have tetrahydro-like spectra (Kaufman, 1961; Bailey & Ayling, 1983).

Of the various possible dihydro structures, only the 7,8- and 5,8-dihydro species have double bonds that are conjugated with the dithiolene C=C bond. This is an important consideration since the Raman excitation wavelength, 676.4 nm, is far from any intrinsic electronic transition of the pterin ring. The long wavelength absorption bands arise from dithiolene−Mo charge transfer transitions (Finnegan et al., 1993). The enhancement of pterin ring modes implies that the pterin ring participates in these transitions. Electronic communication between the pterin and the dithiolene is unlikely in the absence of conjugation.

We therefore infer that the pterin as a 5,8-dihydro species and tentatively assign the strong 1576 cm^{-1} RR band (Figure 5) to the stretching mode of the C(6)=C(7) bond, which is conjugated to the dithiolene in this structure (see Figure 1 for atom numbering). The dithiolene C=C stretch is then assigned to the 1526 cm^{-1} band, close to the dithiolene assignments for I and II. This pair of bands, which dominates the high-frequency DRox spectrum, represents the coupled motions of the dithiolene−pterin conjugated double bonds.

The absence of significant enhancement of high-frequency RR bands in DRred (Figure 5) might be due to stabilization of a different dihydro form but is more likely simply a result of altered resonance conditions. The lowest energy absorption band is significantly blue-shifted in DRred relative to DRox (Figure 2), no doubt reflecting the altered d orbital occupancy of Mo[IV]. The excitation wavelength, 676.4 nm, is therefore somewhat off-resonance for DRred. Although significant enhancement is nevertheless observed for low-frequency bands, the high-frequency band enhancement may be insufficient for detection. We tried excitation at shorter wavelengths but encountered excessive interference from fluorescence.

(4) Mo−S Vibrations and Pterin Coupling. In the low-frequency region, the RR spectra are strikingly homologous in two respects, for both oxidation states of the protein and for both model compounds: (a) a band at 350 cm^{-1} shifts 6−8 cm^{-1} on ^{34}S incorporation, identifying it as a mainly Mo−S stretching vibration, and (b) several other bands are ^{34}S-sensitive to a lesser extent, showing the Mo−S coordinate to mix extensively into other modes of the chromophore. Since the chromophore in I and II is the Mo−dithiolene chelate, conjugated with pterin or quinoxaline, this similarity in the vibrational pattern provides strong support for the proposal that the protein also contains a pterin-conjugated Mo−dithiolene chelate. Alternative modes of Mo binding (Enemark & Young, 1993), e.g., chelation by pterin O and N atoms or binding to only one S atom of the pterin side chain, are less likely.

It is possible that additional sulfur atoms, from cysteine or methionine side chains, are bound to the Mo in the protein (Cramer, 1983). These would give rise to additional Mo−S stretches. Substantial resonance enhancement is unlikely for these modes, however (Subramanian et al., 1990), because thiolate−Mo charge transfer transitions are expected near 400 nm, far from the 676.4 nm excitation wavelength. Other than the 350 cm^{-1} band, no bands are seen in the protein spectra which show large ^{34}S shifts, although additional Mo−S stretches are expected to do so since the isotope should have been incorporated into all S atoms of the protein.

Considering the Mo−dithiolene chelate structure in isolation, one would expect two stretching vibrations associated with the Mo−S bonds, in the 300−400 cm^{-1} region, a symmetric and an asymmetric combination of the Mo−S coordinates. A previous RR study of Mo−dithiolene complexes showed resonance enhancement for only a single band in this frequency region, at 365 cm^{-1} for $Mo^{IV}[S_2C_2-(CO_2Me)_2]_3^{2-}$ and at 393 cm^{-1} for $Mo^{IV}O[S_2C_2(CO_2Me)_2]_2^{2-}$ (Subramanian et al., 1990). These bands were assigned to the Mo−S symmetric stretching modes. The 350 cm^{-1} of the protein and model compound spectra is likewise assigned to the symmetric stretch. The normal mode calculation on II shows the Mo−S bonds to stretch in phase in the eigenvector of the 350 cm^{-1} mode, while the out-of-phase combination mixes with several other modes. It is remarkable that the Mo−S stretching frequency is the same in all four species examined here, implying the same Mo−S bond strength, and therefore the same electron density on Mo, despite the differences in ligation and oxidation state. DRred contains Mo[IV], as do I and II. Besides the dithiolene chelate, the ligands in the model compounds are a pair of cyclopentadienide rings, while in DRred, the Mo is probably bound to an oxo and a hydroxy group, as well as to two or more protein side chains. Collectively, this ligand set seems to have the same donor strength as the two cyclopentadienide

ligands. Oxidation to DRox probably converts the hydroxy ligand to a second oxo ligand, on the basis of EXAFS results for other MPT proteins (George et al., 1989, 1990; Cramer et al., 1984). The oxo ligand is a better π donor (Subramanian et al., 1990), and the resulting increase in electron density evidently compensates for the loss of two electrons from the Mo valence shell.

The normal coordinate analysis of **II**, which successfully models the distribution of ^{34}S isotope shifts, indicates that the numerous additional low-frequency bands have contributions from a variety of deformation coordinates, including those of the quinoxaline ring. Enhancement of these modes could result in part from the vibrational coupling to the Mo−S coordinates, but this mechanism is insufficient to explain the ring mode intensities for **I** and **II**, since several of these are much greater than the 350 cm^{-1} band intensity. For these, as for the high-frequency ring modes, the enhancement mechanism must involve electronic participation of the pterin and quinoxaline rings in the Mo−dithiolene charge transfer transitions.

The low-frequency ring mode intensities are much lower in the spectra of the proteins, probably reflecting the more limited conjugation available to the dihydropterin. In DRox, the 350 cm^{-1} Mo−S band is the strongest band in the low-frequency spectrum, while in DRred the intensities are comparable for the 350 cm^{-1} mode and for several ring modes. It appears that conjugation is somewhat greater for DRred than for DRox, possibly reflecting a conformational change that brings the pterin closer to coplanarity with the dithiolene ring.

CONCLUSIONS

RR spectroscopy of DR, in conjunction with the pterin and quinoxaline model compounds, establishes that (1) Mo is bound to pterin via a dithiolene chelate, characterized by an Mo−S symmetric stretching mode at 350 cm^{-1}, and (2) pterin modes in the 200−400 cm^{-1} region are vibrationally coupled with the Mo−S stretches; their enhancement in RR spectra excited at long wavelengths imply pterin participation in the resonant charge−transfer transitions via conjugation with the dithiolene. The dithiolene C=C stretching vibration is tentatively identified at 1506 and 1515 cm^{-1} in the model compounds, and at 1526 cm^{-1} in DRox. A strong DRox RR band at 1576 cm^{-1} is suggested to arise from stretching of the C(6)=C(7) conjugated double bond in the 5,8-dihydro form of the pterin in the native cofactor.

REFERENCES

Bailey, S. W., & Ayling, J. E. (1983) *Biochemistry 22*, 1790. .

Bastian, N. R., Kay, C. J., Barbara, N. J., & Rajagopalan, K. V. (1991) *J. Biol. Chem. 266*, 45.

Bordas, J., Bray, R. C., Garner, C. D., Gutteridge, S., & Hasnain, S. S. (1980) *Biochem. J. 191*, 495.

Branzoli, U., & Massey, V. (1974) *J. Biol. Chem. 249*, 4346.

Brown, D. J. (1988) in *Fused Pyrimidines*, Part Three, pp 416−426, John Wiley and Sons, New York.

Clark, R. J. H., & Turtle, P. C. (1978) *J. Chem. Soc., Dalton Trans.*, 1714.

Cramer, S. P. (1983) *Adv. Inorg. Bioinorg. Mech. 2*, 259.

Cramer, S. P., & Hille, R. (1985) *J. Am. Chem. Soc. 107*, 8164.

Cramer, S. P., Gray, H. B., & Rajagopalan, K. V. (1979) *J. Am. Chem. Soc. 101*, 2772.

Cramer, S. P., Wahl, R., & Rajagopalan, K. V. (1981) *J. Am. Chem. Soc. 103*, 7721.

Cramer, S. P., Solomonsen, L. S., Adams, M. W., & Mortenson, L. E. (1984) *J. Am. Chem. Soc. 106*, 1467.

Czernuszewicz, R. S. (1986) *Appl. Spectrosc. 40*, 571.

Czernuszewicz, R. S., & Johnson, M. K. (1983) *Appl. Spectrosc. 37*, 297.

Enemark, J. H., & Young, C. G. (1993) *Adv. Inorg. Chem. 40*, 1.

Finnegan, M. T., Hilton, J., Rajagopalan, K. V., & Johnson, M. K. (1993) *Inorg. Chem. 32*, 2616.

Fodor, S., Rava, R. P., Hays, T. R., & Spiro, T. G. (1985) *J. Am. Chem. Soc. 107*, 1520.

Gardlik, S., & Rajagopalan, K. V. (1990) *J. Biol. Chem. 265*, 13047.

George, G. N., Kipke, C. A., Prince, R. C., Sunde, R. A., Enemark, J. H., &

Cramer, S. P. (1989) *Biochemistry 28*, 5075.

George, G. N., Cleland, W. E., Jr., Enemark, J. H., Smith, B. E., Kipke, C. A., Roberts, S. A., & Cramer, S. P. (1990) *J. Am. Chem. Soc. 112*, 2541.

Gruber, S., Kilpatrick, L., Bastian, N. R., Rajagopalan, K. V., & Spiro, T. G. (1991) *J. Am. Chem. Soc. 112*, 8179.

Hille, R., & Sprecher, H. J. (1987) *J. Biol. Chem. 262*, 10914.

Hille, R., George, G. N., Eidness, M. K., & Cramer, S. P. (1989) *Inorg. Chem. 28*, 4018.

Holm, R. (1990) *Coord. Chem. Rev. 110*, 183.

Johnson, J. L., & Rajagopalan, K. V. (1982) *Proc. Natl. Acad. Sci. U.S.A. 79*, 6856.

Johnson, J. L., Hainline, B. E., & Rajagopalan, K. V. (1980) *J. Biol. Chem. 255*, 1783.

Johnson, J. L., Hainline, B. E., Rajagopalan, K. V., & Arison, B. H. (1984) *J. Biol. Chem. 259*, 5414.

Johnson, J. L., Bastian, N. R., & Rajagopalan, K. V. (1990) *Proc. Natl. Acad. Sci. U.S.A. 87*, 3190.

Kaufman, S. (1961) *J. Biol. Chem. 236*, 804.

Kim, J., & Rees, D. C. (1992) *Nature 316*, 553.

Kim, J., & Rees, D. C. (1994) *Biochemistry 33*, 389.

Kramer, S. P., Johnson, J. L., Ribeiro, A. A., Millington, D. S., & Rajagopalan, K. V. (1987) *J. Biol. Chem. 262*, 16357.

Matsura, S., Murata, S., & Sugimoto, T. (1986) in *Chemistry and Biology of Pteridines* (Cooper, B. A., & Whitehead, V. M., Eds.) p 81, de Gruyter, Berlin, Germany.

Müller, A., Jostes, R., Eltzner, W., Nie, C.-S., Dieman, E., Bösse, H., Zimmerman, M., Dartmann, M., Reinsch-Vogell, U., Che, S., Cyvin, S. J., & Cyvin, B. N. (1985) *Inorg. Chem. 24*, 2872.

Nason, A., Lee, K.-Y., Pan, S.-S., Ketchum, P. A., Lamberti, A., & de Vries, K. (1971) *Proc. Natl. Acad. Sci. U.S.A. 68*, 3242.

Pilato, R. S., Eriksen, K. A., Greaney, M. A., Stiefel, E. I., Goswami, S., Kilpatrick, L., Spiro, T. G., Taylor, E. C., & Rheingold, A. L. (1991) *J. Am. Chem. Soc. 113*, 9372.

Pilato, R. S., Eriksen, K., Greaney, M. A., Gea, Y., Taylor, E. C., Goswami, S., Kilpatrick, L., Spiro, T. G., Rheingold, A. L., & Stiefel, E. I. (1993) in *Molybdenum Enzymes, Cofactors, and Model Systems* (Stiefel, E. I., Coucovanis, D., & Newton, W. E., Eds.) Chapter 6, ACS Symposium, Washington, D.C.

Rajagopalan, K. V. (1991) *Adv. Enzymol. Relat. Areas Mol. Biol. 64*, 215−290.

Randles, D., & Armarego, W. L. F. (1985) *Eur. J. Biochem. 146*, 467.

Satoh, T., & Kurihara, F. N. (1987) *J. Biochem. (Tokyo) 102*, 191.

Schachtschneider, J. H. (1962) Shell Development Co., Technical Report No. 263-263.

Schläpfer, C. W., & Nakamoto, K. (1975) *Inorg. Chem. 14*, 1338.

Scully, D. B., & Whiffen, D. H. (1960) *Spectrochim. Acta 16*, 1409.

Subramanian, P., Burgmayer, S., Richards, S., Salai, V., & Spiro, T. G. (1990) *Inorg. Chem. 29*, 3849.

Turner, N. A., Bray, R. C., & Diakun, G. P. (1989) *Biochem. J. 26*, 563.

Viscontini, M. (1971) *Methods Enzymol. 18B*, 678.

Wilson, E. B., Decius, J. C., & Cross, J. C. (1955) in *Molecular Vibrations*, McGraw Hill, New York.